J|A|C|S
ARTICLES
Published on Web 05/12/2007

trans-W(Cmesityl)(dmpe)$_2$H: Revealing a Highly Polar W−H Bond and H-Mobility in Liquid and Solid State

Fenglou Zou,[†] Franck Furno,[†] Thomas Fox,[†] Helmut W. Schmalle,[†] Heinz Berke,*[,†] Jürgen Eckert,*[,‡,§] Zema Chowdhury,[||] and Peter Burger[‡,⊥,||]

Contribution from the Anorganisch-chemisches Institut, Universität Zürich, Winterthurerstrasse 190, CH-8057 Zürich, Switzerland, LANSCE-LC, Los Alamos National Laboratory, Los Alamos, New Mexico 87545, Materials Research Laboratory, University of California, Santa Barbara, California 93106, and NIST Center for Neutron Research, Bldg 235, Gaithersburg, Maryland 20899

Received January 10, 2007

Abstract: The isotopomeric complexes *trans*-W(Cmesityl)[(C(H,D)$_3$)$_2$PCH$_2$CH$_2$P(C(H,D)$_3$)$_2$]$_2$(H,D) **1**−**4** were prepared. **2** (W(C$_{mesityl}$)(dmpe)$_2$D) was used to study the Deuterium Quadrupole Coupling Constant (DQCC) and the ionicity of the W−D bond (DQCC = 34.1 kHz; ionicity 85%). **1** (W(C$_{mesityl}$)(dmpe)$_2$H) shows several dynamic exchange processes in solution, such as H$_W$/H$_W$, H$_W$/*ortho*-Me$_{mesityl}$, and H$_W$/H$_2$ exchanges observed by NMR in combination with deuterium labeling studies and double label crossover experiments. Except for the H$_W$/H$_2$, these reactions comprise elementary steps, which also appear along the isomerization pathway of **1** into (2,3,5-trimethylphenylcarbyne)(dmpe)$_2$WH (**5**) at 60 °C. **5** was characterized by an X-ray diffraction study. In the solid state only an H$_W$/Me$_p$ exchange process prevails appearing at higher temperatures, which was identified by NMR and by Quasielastic Neutron Scattering. The latter also provided an activation barrier of 5 kcal/mol and a "jump width" for the moving H nucleus in agreement with the H$_W$···Me$_p$ distance of the X-ray diffraction study of **1**.

Transition metal hydride (TMH) complexes[1] are viewed as the key components in a variety of organometallic transformations and catalytic schemes, during which they insert a wide range of unsaturated compounds into the TMH bonds.[2] In mechanistic terms many of these insertion steps are not, however, insertions in the sense of intramolecular H shifts at the metal center but rather comprise in their intimate part hydride transfers to appropriate electrophiles.[3] This may even be the preferred route of TMH complexes with enhanced hydride donor abilities of the TM−H bond.[4] However, a free H$^-$ ion has never been observed in such reactions or detected in solution, so that any research finding to this end would be of considerable importance.

We have recently prepared various TMH complexes with strong hydridic polarizations in the TMH bonds. One of these compounds is *trans*-W(CMes)(dmpe)$_2$H (dmpe = 1,2-bis-(dimethylphosphino)ethane) **1**.[5] The synthesis, full characteriza-

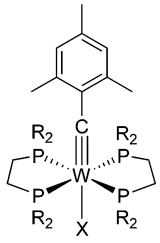

X = H, R = CH$_3$ **1**; R = CD$_3$ **3**
X = D, R = CH$_3$ **2**; R = CD$_3$ **4**

tion, and insertion type reactivity of **1** toward small unsaturated organic and inorganic molecules have been reported elsewhere.[5] These studies, together with density functional calculations,[6]

[†] Universität Zürich.
[‡] Los Alamos National Laboratory.
[§] University of California.
[||] NIST Center for Neutron Research.
[⊥] Present address: Institut für Anorganische Chemie, Universität Hamburg, Martin-Luther-King-Platz 6, D-20146 Hamburg, Germany.

(1) Kubas, G. J. *Metal Dihydrogen and σ-Bond Complexes*; Kluwer, Academic/Plenum: New York, 2001.
(2) For example, see: (a) *Houben-Weyl Methoden der Organischen Chemie*; Georg Thieme Verlag: Stuttgart, Germany, 1981; Vol. IV/1d, pp 267−282, 293−338; 1984; Vol. IV/1b, pp 141−288. (b) Collman, J. P.; Hegedus, L. S.; Norton, J. R.; Finke, R. G. *Principles and Applications of Organotransition Metal Chemistry*; University Science Books: Mill Valley, CA, 1987; Chapter 10. (c) Ojima, I.; Eguchi, M.; Tzamarioudaki, M. In *Comprehensive Organometallic Chemistry II*; Abel, E. W., Stone, F. G. A., Wilkinson, G., Eds.; Pergamon: Exeter, 1995; Vol. 12, Chapter 2. (d) Berke, H.; Burger, P. *Comments Inorg. Chem.* **1994**, *16*, 279.
(3) (a) Gaus, P. L.; Kao, S. C.; Youngdahl, K.; Darensbourg, M. Y. *J. Am. Chem. Soc.* **1985**, *107*, 2428. (b) Collman, J. P.; Wagenknecht, P. S.; Lewis, N. S. *J. Am. Chem. Soc.* **1992**, *114*, 5665. (c) Hembre, R. T.; McQueen, S. *J. Am. Chem. Soc.* **1994**, *116*, 2141. (d) Bullock, R. M.; Song, J.-S. *J. Am. Chem. Soc.* **1994**, *116*, 8602. (e) Luan, L.; Song, J.-S.; Bullock, R. M. *J. Org. Chem.* **1995**, *60*, 7170. (f) Voges, M. H.; Bullock, R. M. *J. Chem. Soc., Dalton Trans.* **2002**, 759. (g) Song, J.-S.; Szaldo, D. J.; Bullock, R. M. *Inorg. Chim. Acta* **1997**, *259*, 161. (h) Cheng, T. Y.; Bullock, R. M. *Organometallics* **2002**, *21*, 2325.
(4) Jacobsen, H.; Berke, H. *Recent Advances in Hydride Chemistry*; Poli, R., Ed.; Elsevier: Amsterdam, 2001; p 89.
(5) (a) Furno, F.; Fox, T.; Schmalle, H. W.; Berke, H. *Organometallics* **2000**, *19*, 3620. (b) Furno, F.; Fox, T.; Alfonso, M.; Berke, H. *Eur. J. Inorg. Chem.* **2001**, 1559. (c) Furno, F.; Fox, T.; Schmalle, H. W.; Berke, H. *Chimia* **1999**, *53*, 350.
(6) Jacobsen, H.; Berke, H. *J. Chem. Soc., Dalton Trans.* **2000**, 3117.

have indeed indicated an enhanced hydridic character, mainly due to the design of the hydride complex bearing strong *σ*-donating phosphines and a mesityl carbyne ligand in *trans* position, which is known to exert a strong *trans*-influence/effect.[7] A X-ray diffraction analysis[5a] of **1** demonstrated that the overall geometry about the tungsten center is that of a slightly distorted octahedron with a distance for the W−H bond of 2.0 Å, while DFT calculations revealed a W−H distance of 1.88 Å. Both results point to a long and relatively weak TM−H bond.[6]

On the basis of these structural properties and the high activity in H-transfer reactions, it was not too surprising to find a very high value of the W−H bond ionicity determined by two different techniques. VT ^{2}H-T_1 NMR relaxation times were determined in toluene-d_8 solution for the deuterium labeled compound **2**, which were used for the calculation of the deuterium quadrupole coupling constant (DQCC) and the ionic bond character (*i*) in the covalent W−H bond.[8] The rate of ^{2}H spin−lattice relaxation is dominated by quadrupolar interactions. **2** shows a broad multiplet at $\delta = -6.60$ ppm in its ^{2}H NMR spectrum. The logarithmic ^{2}H-T_1 times of the ^{2}H resonance for the D ligand of **2** measured at 213 K (76.7 MHz) and plotted as a function of 1/T were used to extract a T_1 min value of 59 ms, which corresponds to a DQCC of 34.1 kHz and (*i*) = 85%[9,10] calculated from (*i*) = 1-(DQCC/227).[9] We have also employed solid-state ^{2}H NMR as an alternative technique to evaluate the DQCC in **2**[10] whereby the DQCC can be directly extracted from the Pake doublet splitting.[11] A similar value of 34.8 kHz for the DQCC was found in nice agreement with the liquid ^{2}H-T_1 measurement. The degree of W−D bond ionicity in **2** of about 85% is higher than values reported for $(CO)_5MnD$ ((*i*) = 70%), Cp_2WD_2 ((*i*) = 76%), $WD(NO)(CO)_2(PMe)_2$ ((*i*) = 79%), Cp_2ZrD_2 ((*i*) = 79%), $WD(NO)(CO)(PMe)_3$ ((*i*) = 82%),[9] and $MoD(NO)(dmpe)_2$ ((*i*) = 84%).[12] The smallest known experimental DQCC value, 33 kHz, (*i*) = 85%, is that of the LiD molecule,[13] which is close to our results for the *trans*-$W(CMes)(dmpe)_2D$ complex, which approaches the ionic limit of an M−D bond with a zero DQCC value. On the other hand a DQCC value of 227 kHz in HD[14] represents the 100% covalent end of the scale. The solid state measurements in addition revealed a very long relaxation time for the metal bound deuteride (T_1 = 300 s (298 K)) and did not indicate any intermolecular exchange at this temperature.[11,15]

Scheme 1

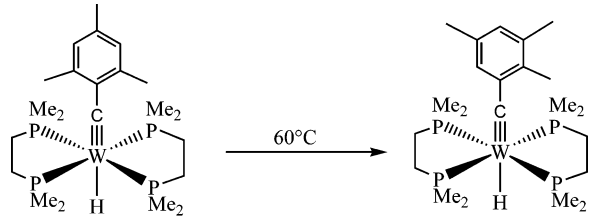

1 **5**

Isomerization of 1 into W[(C(TMP)](dmpe)$_2$H (TMP = 2,3,5-Trimethylphenyl) (5). At 60 °C W(CMes)(dmpe)$_2$H (**1**) was observed to rearrange within 2 weeks to form W[(C(TMP)]-(dmpe)$_2$H (TMP = 2,3,5-trimethylphenyl) (**5**) in benzene or toluene solution with a 90% spectroscopic yield of **5** (isolated yield 71%) (Scheme 1).

The isomerization was first thought to be initiated by light. However, a UV irradiation experiment with a mercury lamp (125 W) in a cold water bath did not reveal any changes.

The ^{1}H NMR spectrum of **5** displays a quintet for the hydride ligand at −5.62 ppm ($^2J_{PH}$ = 35 Hz, J_{WH} = 34 Hz) about 1 ppm at lower field than that of **1**. The rearrangement of the aromatic ring becomes also obvious in the ^{1}H NMR spectrum, since **5** shows for the Me_{Ar} groups three singlets of equal intensity. In the aromatic chemical shift region two distinct resonances are detected assigned to the two nonequivalent H_{Ar} atoms. The ^{31}P NMR spectrum indicated equivalence of all four phosphorus nuclei showing a singlet at 25.6 ppm (J_{WP} = 276 Hz), which is shifted about 0.5 ppm to lower field in comparison with **1**.

The spectroscopically derived structure of **5** was eventually confirmed by a single-crystal X-ray diffraction study. Red single crystals were grown by cooling a hexane solution to −35 °C. The ORTEP plot of **5** is shown in Figure 1. Selected bond lengths and bond angles are listed in Table 1.

In the X-ray diffraction study the $H_{hydride}$ ligand (H49) was found in a difference Fourier map. Its coordinates were kept fixed, and the isotropic displacement parameters were refined. All other positions of H-atoms were recalculated after each refinement cycle.

As shown in Figure 1, **5** possesses a similar structure to that of **1** with a square bipyramidal geometry of the heavy atoms around the tungsten center with four phosphorus atoms in the quasi equatorial plane, while the $H_{hydride}$ atom and the carbyne ligand are located perpendicular to that plane in *trans* positions similar to the structure of **1**.

The structural data of **5** can be interpreted in terms of reduced molecular strain in comparison with **1**. For instance, as listed in Table 1, the W(1)−C(13) bond length of **5** is 1.838(9) Å, which is significantly shorter than the corresponding bond of **1** (1.863(6) Å). Presumably this shortening is due to less non-bonding contacts between the Me_{Ar} and Me_{dmpe} groups (closest distance of **5** 2.519 Å). The presence of $Me_{Ar}\cdots Me_{dmpe}$ steric repulsion can also be derived from the C(14)−C(13)−W(1) "hinging" angle of the aromatic ring of **5** (174.7(7)°) bending

(7) Appleton, T. G.; Clark, H.; Manzer, L. *Coord. Chem. Rev.* **1973**, *10*, 335. Atwood, J. D. *Inorganic and Organometallic Reaction Mechanisms*, 2nd ed.; VCH Publishers: New York, 1997. Shriver, D. F., Atkins, P. W., Eds. *Inorganic Chemistry*; W. H. Freeman and Co: New York, 1999. Basolo, F.; Pearson, R. G. *Progr. Inorg. Chem.* **1962**, *4*, 381. Faller, J. W.; Lambert, C.; Mazzieri, M. R. *J. Organomet. Chem.* **1990**, *383*, 161. Faller, J. W.; Mazzieri, M. R.; Nguyen, J. T.; Parr, J.; Tokunaga, M. *Pure Appl. Chem.* **1964**, *66*, 1463.
(8) (a) Nietlispach, D.; Bakhmutov, V. I.; Berke, H. *J. Am. Chem. Soc.* **1993**, *115*, 9191. (b) Gusev, D. G.; Nietlispach, D.; Vymenits, A. B.; Bakhmutov, V. I.; Berke, H. *Inorg. Chem.* **1993**, *32*, 3270. (c) Wharton, L.; Gold, L. P.; Klemperer, W. *J. Chem. Phys.* **1962**, *37*, 2149.
(9) (a) Fee, F. W.; Chan, M. C. W.; Cheung, K. K.; Che, C. M. *J. Organomet. Chem.* **1998**, *563*, 191. (b) Zhang, L.; Gamasa, M. P.; Gimeno, J.; Carbajo, R. J.; Lopez-Ortiz, F.; Lanfranchi, M.; Tiripicchio, A. *Organometallics* **1996**, *15*, 4274.
(10) (a) Fyfe, C. A. *Solid State NMR for Chemists*; C.F.C. Press: Ontario, 1983. (b) Dixon, M.; Overill, R. E.; Platt, E. *J. Mol. Struct.* **1978**, *48*, 115. (c) Soda, G.; Chiba, T. *J. Chem. Phys.* **1969**, *50*, 439. (d) Butler, L. G.; Brown, T. L. *J. Am. Chem. Soc.* **1981**, *103*, 6541. (e) Kim, A.; Fronczek, F. R.; Butler, L. G.; Chen, S.; Keiter, E. A. *J. Am. Chem. Soc.* **1991**, *113*, 9090.
(11) Smith, J. A. S. *J. Chem. Educ.* **1971**, *48*, 39.
(12) Liang, F.; Schmalle, H. W.; Fox, T.; Berke, H. *Organometallics* **2003**, *22*, 3393.
(13) (a) Wei, Y.; Fung, B. M. *J. Chem. Phys.* **1971**, *55*, 1486. (b) Ireland, P. S.; Olson, L. W.; Brown, T. L. *J. Am. Chem. Soc.* **1975**, *97*, 3548. (c) Jarrett, W. L.; Farlee, R. D.; Butler, L. G. *Inorg. Chem.* **1987**, *26*, 1381.
(14) Guo, K.; Jarrett, W. L.; Butler, L. G. *Inorg. Chem.* **1987**, *26*, 3001.
(15) Hayashi, S. *Inorg. Chem.* **2002**, *41*, 2238. Hayashi, S. *J. Phys. Chem. Solids* **2003**, *64*, 2227. Hayashi, S. *J. Solid State Chem.* **2003**, *170*, 82. Hayashi, S. *J. Alloy Compd.* **2002**, *330*, 443.

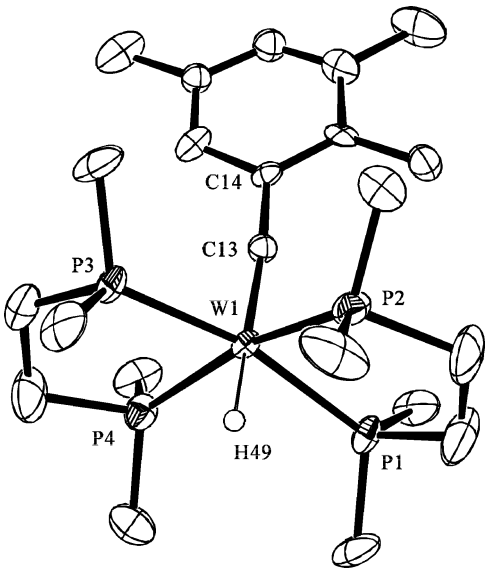

Figure 1. ORTEP plot of **5** with thermal ellipsoid probabilities of 50%. All H atoms except for H49 are omitted for clarity.

Table 1. Selected Bond Lengths (Å) and Bond Angles (deg) for **5**

Bond lengths			
W(1)−C(13)	1.838(9)	W(1)−P(4)	2.429(3)
W(1)−P(3)	2.412(3)	W(1)−P(1)	2.436(3)
W(1)−P(2)	2.420(3)	W(1)−H(49)	1.62
Bond angles			
C(13)−W(1)−H(49)	168.1(3)	C(13)−W(1)−P(3)	93.1(3)
C(13)−W(1)−P(2)	98.5(3)	P(3)−W(1)−P(2)	96.97(11)
C(13)−W(1)−P(4)	98.1(3)	P(3)−W(1)−P(4)	81.19(11)
P(2)−W(1)−P(4)	163.37(10)	C(13)−W(1)−P(1)	102.4(3)
P(3)−W(1)−P(1)	164.55(9)	P(2)−W(1)−P(1)	80.88(10)
P(4)−W(1)−P(1)	96.47(10)	P(3)−W(1)−H(49)	82.09(8)
P(2)−W(1)−H(49)	71.54(8)	P(4)−W(1)−H(49)	91.85(7)
P(1)−W(1)−H(49)	82.74(7)	C(14)−C(13)−W(1)	174.7(7)

toward the unsubstituted side. In **1** the mentioned repulsive forces are balanced leading to an axially symmetric W≡C−C_{Ar} arrangement. All these observations indicate that **5** is thermodynamically considerably more stabilized than **1**. However, a thermodynamic relaxation process is expected to be topologically complex and must consist of various consecutive elementary steps.

Mechanism for the Rearrangement of 1 into 5. In the following sections we show that the mechanism for the rearrangement of **1** into **5** can be rationalized on the basis of an α-shift of the hydride ligand and a sequence of methyl oxidative additions/reductive eliminations at the electron rich tungsten center. A mechanism is sketched in Scheme 2 including an isotopic labeling scheme to be discussed later.

It was observed earlier that a complex related to **1**, namely *trans*-W(CMes)(H)(CO)([P(OMe)$_3$)]$_3$, is dynamic at room temperature and equilibrates to *cis*-W(CMes)(H)(CO)([P(OMe)$_3$)]$_3$[16] and the isomeric coordinatively unsaturated carbene complex W(CHMes)(CO)[P(OMe$_3$)]$_3$. Based on this knowledge it appears to be very plausible to assume that such equilibria would also exist for **1** at room temperature and hence lead in subsequent steps to **1a** and **1b**. At 60 °C or even somewhat below that temperature reversible oxidative additions of the ortho methyl groups are "turned on" presumably starting from an agostic binding state as in the case of **1d**. The first C−H oxidative addition of Scheme 2 results in the *cis*-hydrido methylene-bridged complex **1e**. All the following oxidative additions and their reversals C−H reductive eliminations are assumed to be associated with a similar activation barrier than the preceding step. Therefore the overall barrier for the transformation of **1** into **5** is set by these C−H activation processes. The hydride ligand of **1e** then migrates onto the $C_{carbene}$ atom (former $C_{carbyne}$) leading to the 16 e$^-$ species **1f**. A subsequent C−H oxidative addition results in the new carbene hydrido complex **1g**. Reductive C−H elimination closes the rearrangement to the TMP isomeric ring system to yield the carbene complex **5b** related to **1b**. As for **1b** and **1a**, **5b** is expected to be in equilibrium with **5a**, the *cis*-isomer of **5**, from which **5** is eventually generated by ligand rearrangement.

Various Inter- and Intramolecular Dynamics of 1 in the Liquid and Solid State. H_W/H_W Exchange at Room Temperature in Solution Traced by a Deuterium Double Labeling Crossover Study Converting 2 and 3 into 1 and 4. In the previous paragraph the rearrangement of **1** into **5** was established consisting of a sequence of different elementary process, which are distinguished by their activation barriers. The room-temperature steps lead to carbene formation from the carbyne unit and the hydride ligand. The resulting 16e$^-$ complex could indeed undergo a reversible "self-trapping" via dimerization with concomitant exchange of the carbene units.

Double ^{2}H-labeled crossover experiments were carried out in toluene at room-temperature variable but approximately equal concentrations of the isotopomers **2** (W(CMes)(dmpe)$_2$D) and **3** (W(CMes)(dmpe-d$_{12}$)$_2$H). The reaction was monitored by high resolution ^{1}H and ^{31}P NMR spectroscopy allowing us to distinguish all the potentially appearing isotopomers **1**−**4**. The observed scrambling indeed proceeded with equilibration into all possible isotopomers (Scheme 3). It should be noted that isotopomers possessing mixed labels in the phosphine ligands were not observed so that a phosphine exchange process can be ruled out.

In the high resolution ^{31}P NMR spectrum the four isotopomers (**1**−**4**) could be distinguished by their different chemical shifts due to significant deuterium isotope effects: **2**, 25.34 ppm (t); **1**, 25.33 ppm (s); **4**, 23.85 ppm (t); **3**, 23.84 ppm (s). Moreover, **1** and **3** can be distinguished in the ^{1}H{^{31}P} NMR spectrum (toluene-h_8) by distinct hydride signals, which are separated by 50 ppb. The presence of **1** and **3** has also been confirmed by a P,H-correlation spectrum with a hydride resonance of **3** in toluene-h_8 at δ −6.67 ppm.

A concentrated mixture of **2** and **3** (15.5 mM) reached equilibrium at room temperature within 8 days, while a mixture of lower concentration (6.5 mM of **2** and **3**) took ca. 46 days for equilibration at under otherwise the same conditions. When a 2.0 mM solution of **2** and **3** was used, exchange became so slow that it was no longer detectable either by ^{1}H or by ^{31}P NMR spectroscopy. All these observations point to an exchange mechanism with a rate-determining bimolecular step.

The McKay equation[18] was applied to the kinetic pursuit of the crossover experiments of **2** and **3** (Figure 2) and an

(16) Bannwart, E.; Jacobsen, H.; Furno, F.; Berke, H. *Organometallics* **2000**, *19*, 3605.

(17) Spivak, G. J.; Caulton, K. G. *Organometallics* **1998**, *17*, 5260.
(18) Espenson, J. H. In *Chemical Kinetics and Reaction Mechanisms*; 2nd ed.; McGraw-Hill Inc.: New York, 1995; pp 55−57.

Scheme 2

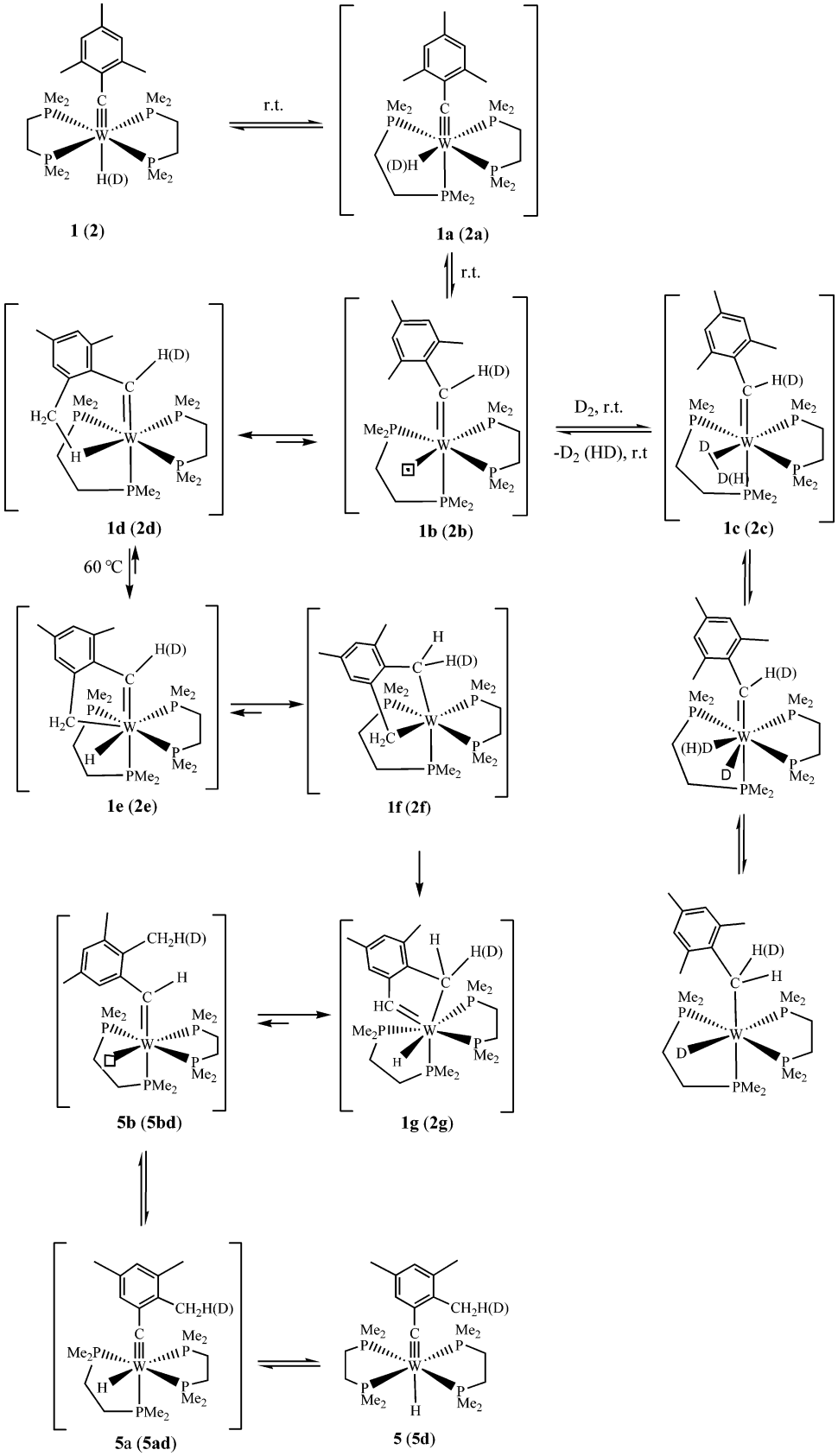

approximate first-order reaction was established as expected for a self-exchange process which is based on the integrations of the signal assigned to **3** at different times. This allowed us to calculate an exchange rate of $R_{ex} = 9.2 \times 10^{-6}$ mol L^{-1} h^{-1} that could be calculated from this relationship. The exchange reaction of **2** and **3** was observed to be even faster at lower temperatures, which again supports an associative reaction mechanism.

Scheme 3

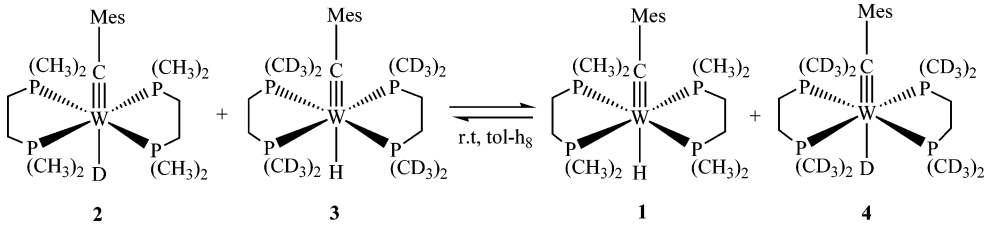

2 **3** **1** **4**

Scheme 4

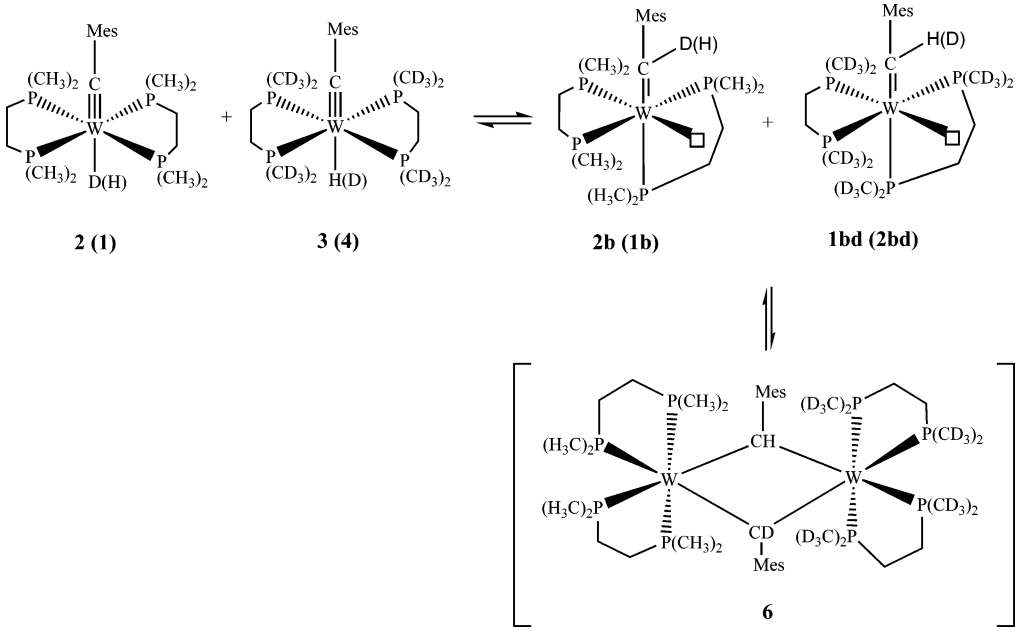

2 (1) **3 (4)** **2b (1b)** **1bd (2bd)** **6**

As proposed in Scheme 4, **2** and **3** would be in equilibrium with the isomeric cis-vacant carbene complex **2b** or **1bd**. Then in a bimolecular step the dinuclear intermediate **6** is expected to be formed via association of these carbene molecules. **1** and **4** would result from the splitting of **6** in a way opposite to which it was formed.

The observed "hydride" H/D exchange is thus not a direct H/D exchange but rather a mediated process of carbene exchanges, which does however stress the existence of carbene intermediates formed by a hydride to carbyne ligand shift (Scheme 2).

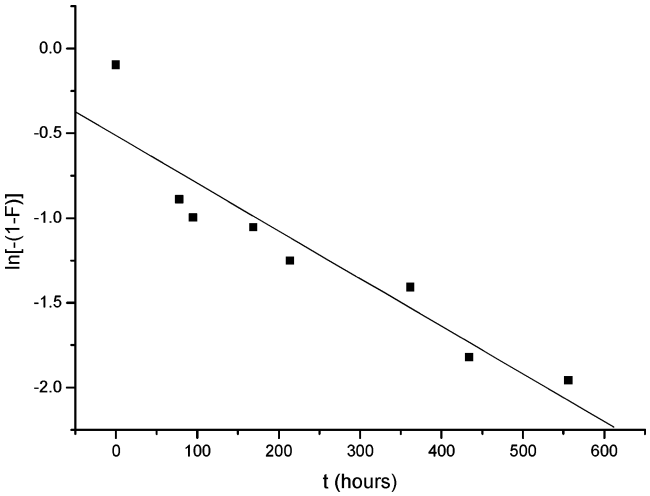

Figure 2. McKay plot for the exchange reaction of **2** and **3** to give **1** and **4** at room temperature (starting concentrations: **2**, 6.5 mM; **3**, 6.3 mM). $^1H\{^{31}P\}$ NMR pursuit of the decay of **2** with the concentration C_t reached at equilibrium state with $C_e = 0.486$ and $F = C_t/C_e$ ($R^2 = 0.93$).

Exchange of 1 with D_2 Gas in Solution at Room Temperature. The occurrence of a carbene intermediate may also be made plausible in an H/D exchange experiment of **1** with D_2 gas. The D_2 molecule traps the carbene complex to form a D_2 complex, which in turn is expected to undergo oxidative addition and subsequent scrambling of metal bound deuterium into the carbene hydrogens via reversible α-migration as sketched in Scheme 2.

The exchange experiments of **1** (W(CMes)(dmpe)$_2$H) with D_2 gas were carried out in solution at various conditions of pressure and temperature. When a solution of **1** was left at room temperature under a pressure of 2 bar of D_2, no apparent H/D exchange according to Scheme 5 was detected even after 10 days. An increase in the D_2 pressure to 60 bar caused the H/D exchange to become noticeable after 6 days, but the amount of **2** formed was minor as verified by ^{31}P and ^2H NMR. Now a

Scheme 5

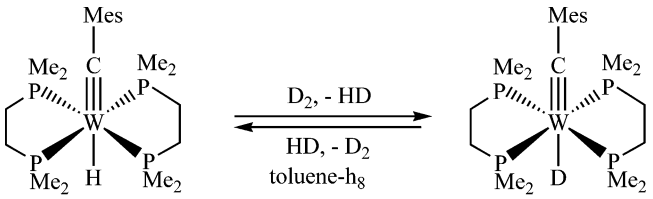

1 **2**

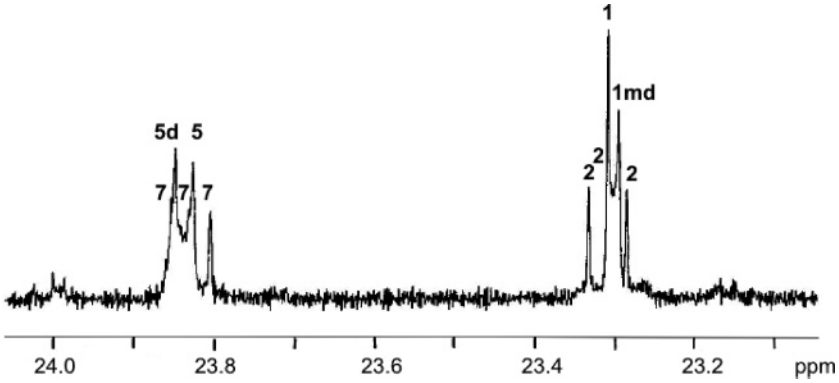

Figure 3. ^{31}P NMR spectrum (toluene-h_8, rt) of the reaction mixture obtained with heating **2** at 60 °C.

Scheme 6

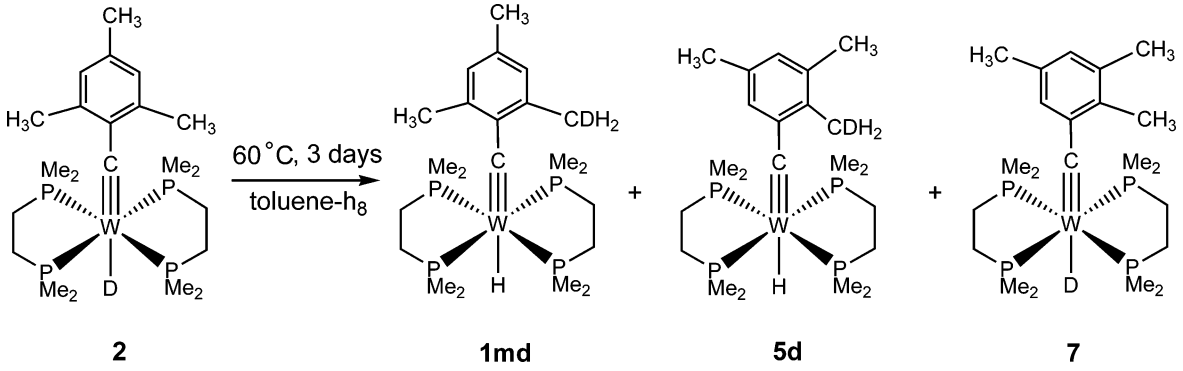

very weak multiplet appearing at −6.62 ppm was then observed in the ^{2}H NMR spectrum.

When a solution of **1** was pressurized with 105 bar of D_2 gas at room temperature and left for 7 days, complete H/D exchange occurred with full conversion into **2** (Scheme 5). While the corresponding hydride resonance for **1** could no longer be found in the ^{1}H NMR spectrum, the ^{2}H NMR spectrum, on the other hand, showed an intense resonance for **2** at −6.57 ppm.

It was then of interest to see if the rearrangement of **1** into **5**, for which the 16e$^-$ carbene intermediate **1b** was also postulated, could be intersected by the reaction with D_2 and equilibrated to the isotopomers of **1** and **5**. Indeed, when a Young tap NMR tube filled with a hexane solution of **1** was pressurized with 2 bar of D_2 gas and the reaction was run at 40 °C in hexane for 10 days, partial H/D exchange occurred to form the deuterides **5d** (W[C(TMP)](dmpe)$_2$D) and **2**. Both species were detected by ^{2}H NMR spectroscopy. A resonance at −5.54 ppm was assigned to **5d** in addition to a quintet at −6.50 ppm belonging to **2**.

Intra- and Intermolecular H/D Exchanges of 1 in Solution at 60 °C. According to Scheme 2 the hydride ligand of **1** would be expected to show at elevated temperatures exchange with the hydrogen atoms of the *ortho*-methyl groups of **1** before it is eventually converted further into **5**.

Indeed, when a solution of **2** was kept in toluene at 60 °C for 3 days, a scrambling of the deuterium content into the *ortho*-methyl groups of the mesityl moiety atom was observed (Scheme 6).

The formation of the products **1md**, **5d**, and **7** given in Scheme 6 was confirmed by NMR spectroscopy. In the ^{1}H NMR spectrum of the isotopic mixture two quintets appear at −5.88 ppm and −6.62 ppm, which were assigned to **5d** and **1md**, respectively. The H_{P-CH_3} resonances of **1md** and **5d** are close to each other at 1.58 and 1.38 ppm.

In the corresponding ^{2}H NMR spectrum two quintets appear at −5.83 and −6.57 ppm, which are assigned to **7** and **2**, respectively. The ^{2}H nucleus of **1md** in the deuterated methyl group of the mesityl moiety appears at 2.50 ppm as a triplet as a result of coupling with the two methylene protons. Likewise, the ^{2}H nucleus of the deuterated methyl group of the TMP ring in **5d** is also assigned a triplet signal at 2.32 ppm because of the same type of coupling. No ^{2}H NMR signal is observed in the possible shift range for P−CDH_2 groups of 1.65 to 1.30 ppm, the possible shift range for P−CDH_2 groups, which would have indicated the presence of H/D exchange into the dmpe ligands.

The intramolecular H/D exchange of **2** is also recognized by ^{31}P NMR spectroscopy on account of differences based on small but significant isotope shifts (Figure 3). A triplet at 23.83 ppm is attributed to **7**, while **5d** gives rise to a singlet at 23.86 ppm; another triplet at 23.30 ppm is assigned to **2**, while the resonance of **1md** appears at 22.29 ppm. Additionally, two additional singlets appear at 23.83 ppm (**5**) and 23.30 ppm (**1**), which are partially overlapping with signals of **7** and **2**, respectively. The formation of **5** and **1** originates from the earlier described room-temperature processes of intermolecular H_W/D_W exchanges of **7** and **2** with any hydride source. These H/D exchange processes would be fully consistent with the pathway shown in Scheme 2 and are expected to occur at the stage of **1f/2f** as the crucial intermediate(s).

Solid-State H-Mobility: Intramolecular H/H or H/D Exchange of 1 or 2 at Elevated Temperatures. The H-mobility in solution described in the previous chapters was in all cases

Scheme 7

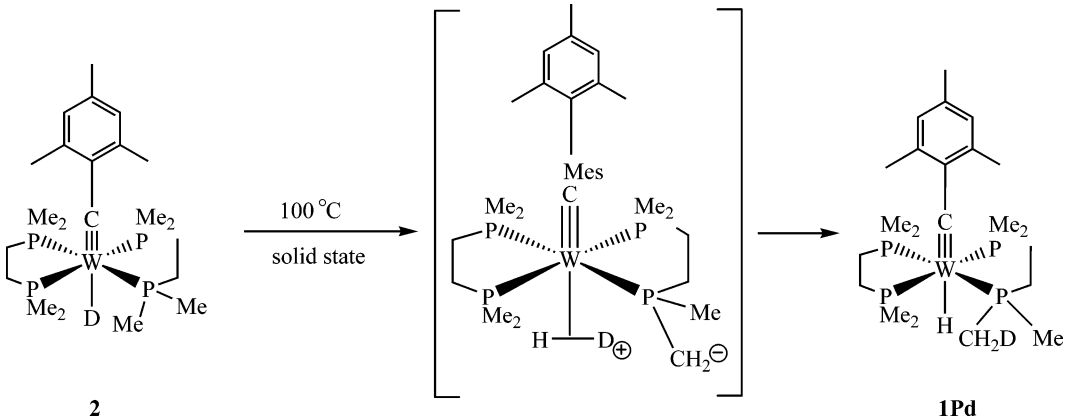

2 **1Pd**

induced by an initial rearrangement of the ligand sphere. Related processes could not be anticipated to occur in the solid state with reasonable activation barriers. If **1** were to exhibit any isomerization with concomitant H-mobility, one would expect this to take place at higher temperatures (>60 °C) and differ from the processes described in the previous chapters.

Indeed, when 5 mg of solid isotopmer **2** was placed into a Young tap NMR tube and then heated to 100 °C for 2.5 h, the room temperature ^{31}P NMR spectrum in toluene-h_8 gave evidence for the formation of a mesitylidyne hydrido tungsten species. The ^{1}H NMR spectrum in toluene-h_8 showed that a complex similar to **1** had formed as indicated by a hydride multiplet at −6.61 ppm. A typical signal was observed at 1.32 ppm in the ^{2}H NMR spectrum which was assigned to monodeuterated P−CH_2D methyl groups. An H/D exchange process according to Scheme 7 was evidently taking place. The solid-state structure of **1** reveals that the shortest distance of H_W to H_{methyl} of the dmpe ligand is approximately 4.25 Å, which indeed is very close to the "jump length" of the Quasielastic Neutron Scattering experiment of **1** (vide infra) are in accord with such an exchange process.

Since the atomic mobility in the solid state is restricted and only hydrogen can normally show dynamic behavior, we have to assume that the mechanism for the rearrangement of **2** into **1Pd** could for instance not be envisaged to take place via oxidative addition of an Me_p group to the tungsten center, because formation of a vacant site would be required. A vacant-site species like **1b** of Scheme 2 cannot be accessed due to a too large degree of necessary topological changes. The pathway of a rearrangement of the dmpe framework possesses however a simple alternative utilizing an intramolecular deprotonation process of **2** with the deuteride ligand as a base. This ligand is expected to show quite a high "gas phase" basicity so that a dmpe methyl group can be deprotonated, perhaps with the help of an appropriate vibrational mode, to form an intermediate dihydrogen complex. This dihydrogen intermediate represents the crucial species for the H/D exchange, and "readdition" of D^+ to the $-CH_2^-$ local anion could complete this exchange. The same rearrangement is anticipated to be the basis of the H-mobility detected in the Quasielastic Neutron Scattering experiment of **1** described below.

H-Mobility Studied by Quasielastic Neutron Scattering. Hydrogen mobility can in principle be readily observed by Quasielastic Neutron Scattering.[19] It was therefore of considerable interest to test if the solid state intramolecular H-mobility described in the previous chapter could be studied in more detail by this method. These measurements would not only give evidence of the presence of such a H/H exchange process, but these data would also provide information on the "jump length" of the mobile H as well as an activation energy for this process when the measurements are carried out as a function of temperature. This seemed possible in a relatively large temperature range, since **1** melts at 433 K.

The technique of Quasielastic Neutron Scattering (QNS) will first of all provide evidence of the H-motion of **1** only if it is sufficiently fast to result in a broadening of the elastic line given by the available neutron scattering spectrometers. This method has been used for a wide variety of related problems such as proton conductors[20] and molecular transport in layer compounds[22] and porous materials.[23] QNS has, however, rarely been used on organometallic compounds except for the observation of reorientational motions of methyl or cyclopentadienyl groups[23] when these are the only H-containing ligands on the metal. The only example of translational proton motion in an organometallic compound observed[24] by QNS has been, to the best of our knowledge, that of H in the exchange of hydride and dihydrogen ligands in the Ir complex $IrClH_2(\eta^2\text{-}H_2)(P\text{-}i\text{-}Pr_3)_2$.

Quasielastic Neutron Scattering data on approximately 2 g of **1** were collected using the High Flux Backscattering Spectrometer at the NIST Center for Neutron Research up to temperatures of 425 K. The energy resolution of the instrument was 1.3 μeV which corresponds to a frequency of about 3×10^8 s^{-1}. Broadening of the quasielastic line was only apparent at temperatures above 300 K. At 150 K we observed quasielastic broadening from the reorientations of the methyl groups, which moved outside the very narrow energy window of this instrument at higher temperatures and, hence, did not affect our results. Quasielastic spectra (summed over all angles) are shown for 25, 400, and 425 K in Figure 4. The angular, or Q

(19) Karmonik, C.; Hempelmann, R.; Matzke, T.; Springer, T. *Z. Naturforsch., A: Phys. Sci.* **1995**, *50*, 539−548.
(20) Poinsignon, C. *Solid State Ionics* **1997**, *97*, 399.
(21) For example, see: Swenson, J. R.; Bergman, W. W.; Howells, S. *J. Chem. Phys.* **2000**, *113*, 2873.
(22) Jobic, H. *J. Phys. IV France* **2000**, *10*, 125.
(23) Bee, M. *Quasielastic Neutron Scattering*; Adam Hilger: Bristol, U.K., 1988.
(24) Raison, P.; Lander, G. H.; Delapalme, A.; Williams, J. H.; Kahn, R.; Carlile, C. J.; Kanellakopolum, B. *Mol. Phys.* **1994**, *81*, 309. Prager, M.; Grimm, H.; Desmedt, A.; Lechner, R. E. *Chem. Phys.* **2003**, *292*, 161.

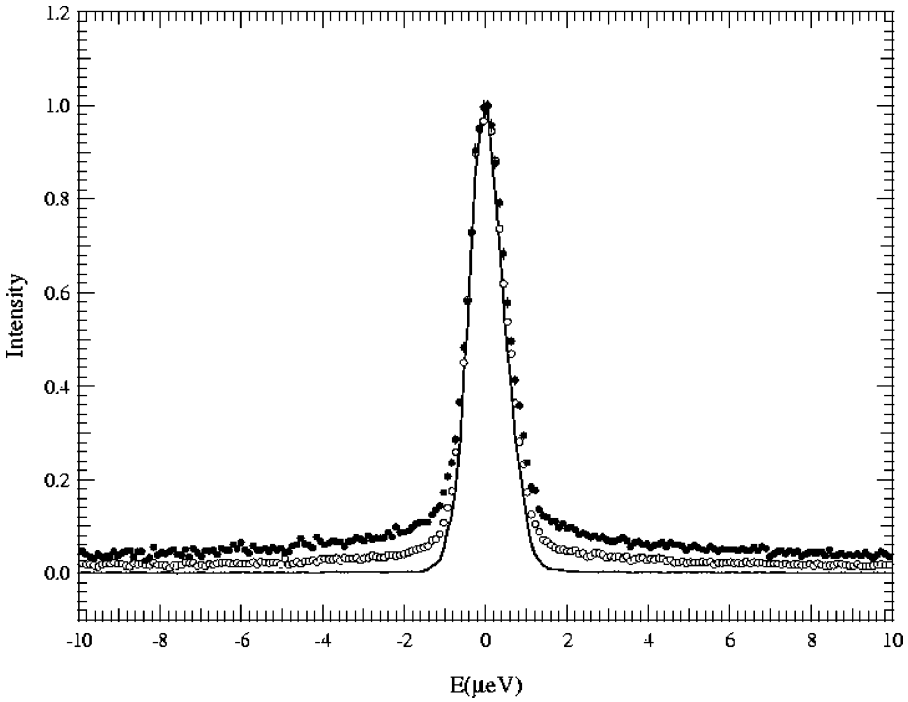

Figure 4. Quasielastic spectra, summed over all angles, for *trans*-W(CMes)(dmpe)$_2$H (**1**) at 25 (—), 400 (○), and 425 K (●).

dependence, of the quasielastic width is shown for the two highest temperatures in Figure 5 along with fits of the two models described below.

The average line width for the three temperatures (where the point at $T = 25$ K is taken to be resolution-limited) can be fit to an Arrhenius law, with the result that the activation energy for this process is about 5 kcal/mol.

We have attempted to fit two common models for jump diffusion[25] to these data, the Chudley−Elliott model with a single jump distance as is commonly used in solids, and one based on a distribution of jump lengths as one would encounter in a liquid. Both models gave similar results with jump lengths between 4.5 and 6.5 Å (Table 2). The residence time τ decreases and the jump length increases from 400 to 425 K.

The single-crystal X-ray diffraction structure shows that the distance of $H_{hydride}$ to $H_{o-methyl}$ of the mesityl group of **1** is 4.25 Å, which obviously matches very well with model 2 of the Quasielastic Neutron Scattering experiments of **1**. The alternative direct "jump" of H_W to $C_{Carbyne}$ to form a carbene complex would amount to only about 3.7 Å. As a "trans jump" it would however have to overcome high kinetic barriers and would not be productive forming new isotopomers from **2**. The generation of **1Pd** from **2** makes it necessary to assume the same process operating in the Quasi Elastic Neutron Scattering Experiment. The low activation barrier found for the solid state rearrangement (5 kcal/mol) is somewhat in contrast to the general experiences that related chemical processes have normally lower activation energies in solution than in solid state. However, for intramolecular H-mobilities this does not always seem to hold.

Finally it should be noted that an intermolecular H_W/H_W self-exchange in the solid state is not supported by the jump length determined from the quasielastic neutron scattering experiment, since the $H_W \cdots H_W$ nonbonding distance is 8.5 Å based on the single-crystal X-ray diffraction study, as well as on a recent single-crystal neutron diffraction study.[26]

Conclusions

A plausible mechanism could be established for the isomerization of **1** into **5** using a variety of specific H/D exchange and double crossover experiments. The reaction is expected to be exothermic due to a release of steric strain. The kinetics of this rearrangement can be separated into room-temperature processes of a ligand sphere rearrangement and a hydride to $C_{Carbyne}$ migration and a series of C−H oxidative addition/reductive elimination processes of the ortho mesityl methyl groups, the latter running at elevated temperature (60 °C). Thermal treatment of **1** at 100 °C in the solid state causes H/H exchange of the hydride ligand with the Me_{dmpe} groups being thus in chemoselectivity different from those processes observed in solution. A Quasielastic Neutron Scattering study of **1** in the solid state confirmed that a H jump exists in the molecule with a distance of 4−5 Å, which approximately matches the H_W to Me_{dmpe} distance (4.25 Å). The rearrangements and intermolecular, as well as intramolecular, exchanges in liquid and in the solid state thus primarily reflect the dynamics of the H_W atom of **1**.

Experimental Section

General. All operations with air-sensitive complexes were performed under an inert atmosphere of N_2 using Schlenk and vacuum line techniques or in a glovebox (Model MB-150B-G). All solvents (including deuterated solvents) were dried and deoxygenated employing appropriate drying/deoxygenating agents and then were newly distillated under nitrogen before use (tetrahydrofuran, toluene, benzene, hexane, pentane, ether, sodium/benzophenone; CH_2Cl_2, P_2O_5, and then CaH_2). IR spectra were obtained on a Bio-Rad FTS instrument. Raman spectra were recorded on a Renishaw Ramanscope spectrometer (514 nm). NMR spectra were recorded on the following spectrometers: Varian

(25) Li, S.; Hall, M. B.; Eckert, J.; Jensen, C. M.; Albinati, A. *J. Am. Chem. Soc.* **2000**, *122*, 2903.

(26) Zou, F.; Albinati, A.; Berke, H. Unpublished results.

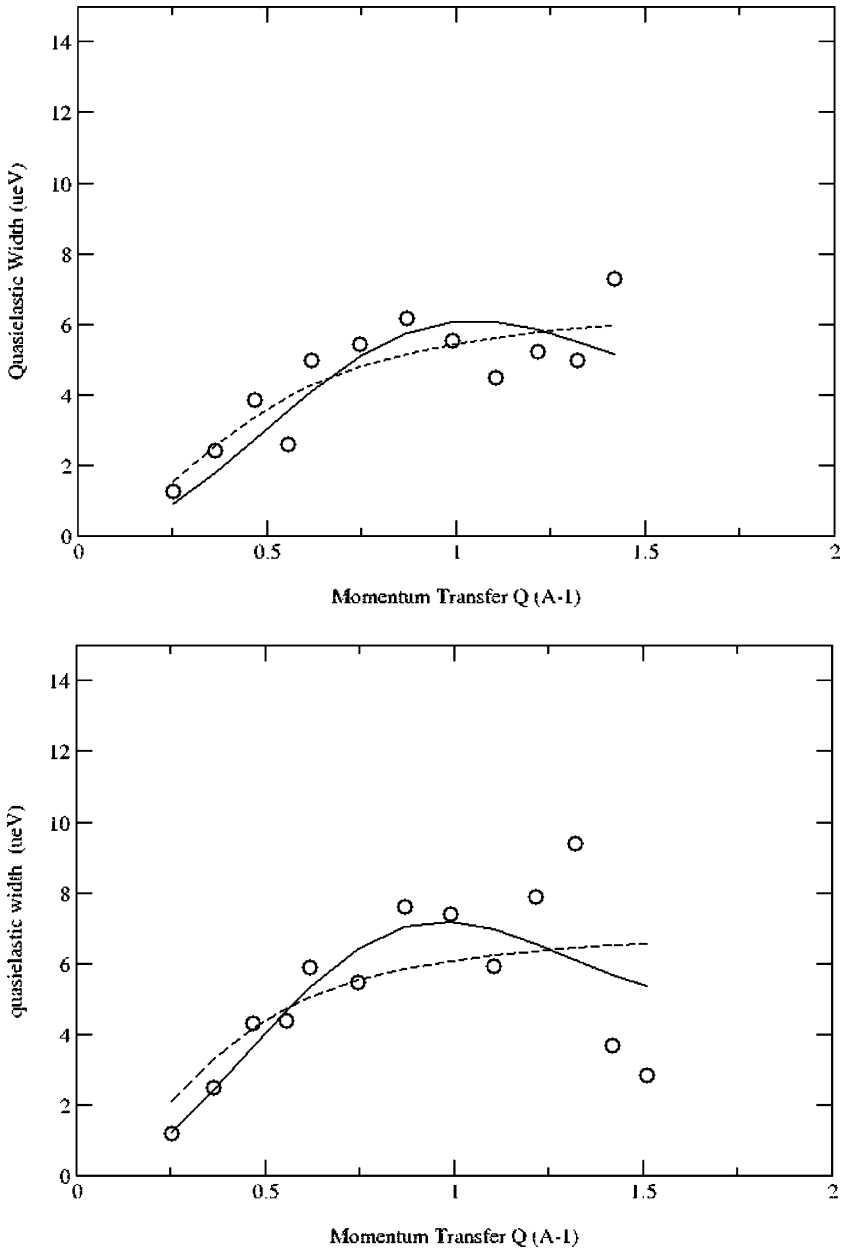

Figure 5. Q-dependence of the quasielastic line widths for *trans*-W(CMes)(dmpe)$_2$H (**1**) at $T = 400$ K (top) and $T = 425$ K (bottom). The fitted lines correspond to the two models for translational diffusion (see Table 2).

Table 2. Results for Fitting the Q-Dependence of the Quasielastic Width to the Singwi−Sjolander (Model 1) and Chudley−Elliott Forms (Model 2) for Translational Diffusion[25]

	model 1		model 2	
T (K)	jump distance (Å)	τ	jump distance (Å)	τ
400	5.6	0.15	4.5	0.2
425	6.4	0.14	4.6	0.17

Gemini-200 instrument (^{1}H at 199.98 MHz, ^{13}C at 50.29 MHz, ^{31}P at 80.95 MHz), Varian Gemini-300 instrument (^{1}H at 300.1 MHz, ^{2}H at 76.7 MHz, ^{13}C at 75.4 MHz, ^{31}P at 121.5 MHz), Bruker DRX-500 instrument (^{1}H at 500.2 MHz, ^{13}C at 125.8 MHz, and ^{31}P at 202.5 MHz). δ (^{1}H) and δ (^{13}C) relative to $SiMe_4$, δ (^{31}P) relative to 85% H_3PO_4, δ (^{11}B) relative to $Et_2O{\cdot}BF_3$. The solid-state NMR measurements have been carried out at −40 °C using a narrow bore probe for 4 mm rotors.

The compounds W(CMes)(dmpe)$_2$H(D)[5a] (**1** and **2**) were synthesized according to the literature. dmpe-d_{12} was prepared in an analogous way to that of dmpe using CD_3I as reagent. W(CMes)(dmpe-d_{12})$_2$H (**3**) was obtained in a way analogous to that for W(CMes)(dmpe)$_2$H using dmpe-d_{12}.

1. Preparation of W(CTMP)(dmpe)$_2$H (TMP = 2,3,5-trimethylphenyl) (5). A solution of 9.2 mg (0.0150 mmol) of W(CMes)(dmpe)$_2$H (**1**) in 0.6 mL of toluene-d_8 in a Young tap NMR tube was heated at 60 °C for 2 weeks. ^{1}H NMR and ^{31}P NMR pursuit demonstrated a 90% spectroscopic yield. After the solvent was removed *in vacuo* the remaining red solid was dissolved in pentane and filtered through Celite. The pentane filtrate was cooled to −35 °C, upon which red crystals of **5** (6.6 mg, 0.0107 mmol) were obtained (yield 71%). Single crystals suitable for a single-crystal X-ray diffraction study were obtained by crystallization from a pentane solution at −35 °C (Table 3).

^{1}H NMR (300 MHz, C_6D_6, 295 K): δ 7.02 (s, 1H, *p*-TMP), 6.73 (s, 1H, *o*-TMP), 2.41 (s, 3H, CH_3—TMP), 2.24 (s, 3H, CH_3—TMP), 2.10 (s, 3H, CH_3—TMP), 1.71 (s, 12H, 4 × CH_3—P), 1.51 (s, 12H, 4 × CH_3—P), 1.55 (m, 8H, 4 × CH_2—P, overlap with one of CH_3—P group),

Table 3. Summary of the X-ray Diffraction Study of **5**

empirical formula	$C_{22}H_{44}P_4W$
formula weight (g·mol^{-1})	616.30
temperature (K)	183(2)
wavelength (Å)	0.710 73
crystal syst, space group	triclinic, $P\bar{1}$
a (Å)	10.0806(9)
b (Å)	12.6747(12)
c (Å)	12.8077(10)
α (deg)	73.376(10)
β (deg)	67.246(9)
γ (deg)	66.989(10)
volume (Å^3)	1371.3(2)
Z, density(calcd) (Mg/m^3)	2, 1.493
abs coefficient (mm^{-1})	4.451
F(000)	620
crystal size (mm^3)	0.23 × 0.05 × 0.02
collection θ range (deg)	2.28 to 25.88
reflections collected	10 799
reflections unique	4983 [R(int) = 0.0823]
θ(max) (deg), completeness to θ (%)	25.88, 93.4
absorption correction	numerical
max/min transmission	0.9027 and 0.7612
data/restraints/parameters	4983/0/241
goodness-of-fit on F^2	0.869
final R indices [$I > 2\sigma(I)$]	R1 = 0.0540, wR2 = 0.1322[a]
R indices (all data)	R1 = 0.0863, wR2 = 0.1400[b]

[a] The unweighted R-factor R1 = $\Sigma(F_{obsd} - F_{calcd})/\Sigma F_{obsd}$. [b] The weighted R-factor wR2 = $\Sigma w(F^2_{obsd} - F^2_{calcd})^2/\Sigma w(F^2_{obsd})^2$.

−5.71 ppm (quintet, 1H, W−*H*, $^2J_{PH}$ = 30 Hz, $^1J_{WH}$ = 30 Hz). ^{31}P NMR (121.48 MHz, C_6D_6, 295 K): δ 25.2 ppm (s, $^1J_{WP}$ = 75.8 Hz). ^{13}C NMR (125.8 MHz, toluene-d_8, 293 K): δ 262.0 (m, 1C, W≡*C*), 155.5 (s, 1C, *ipso*-TMP), 129.2 (s, 1C, *o*-*C*H−TMP), 128.2 (s, 1C, *p*-*C*H−TMP), 136.0 (s, 1C, *o*-*C*−TMP), 132.6 (s, 1C, *m*-*C*−TMP), 130.0 (s, 1C, *m*-*C*−TMP), 36.1 (m, 4C, 4 × *C*H_2−P), 26.6 (m, 4C, 4 × *C*H_3−P), 24.8 (m, 4C, 4 × *C*H_3−P), 21.3 (s, 1C, *C*H_3−TMP), 19.9 (s, 1C, *C*H_3−TMP), 17.2 ppm (s, 1C, *C*H_3−TMP).

Anal. Calcd for $C_{22}H_{44}P_4W$: C, 42.87; H, 7.20. Observed: C, 43.20; H, 7.26.

2. H/D Exchange Reactions. 2.1. Double Label Crossover Experiment Probing H_W/D_W Exchange Using a Solution of 2 and 3 (15.5 mM) at Room Temperature. 0.3 mL of solution of **2** (31.0 mM) in toluene was mixed with 0.3 mL of a solution of **3** with the same concentration in toluene. The H_W/D_W exchange was observed shortly after the solutions of **2** and **3** were mixed. The reaction reached equilibrium within 8 days affording **1** and **4**.

^{31}P{^{1}H}NMR (202.5 MHz, toluene-h_8, rt): **2**, δ 25.34 ppm (t); **1**, δ 25.33 ppm (s); **4**, δ 23.85 ppm (bt); **3**, δ 23.84 ppm (bs).

^{1}H{^{31}P} NMR (500.0 MHz, toluene-h_8, rt): **1**, δ −6.61 ppm (s, H_W); **3**, δ −6.66 ppm (s, H_W).

2.2. Double Label Crossover Experiment Probing H_W/D_W Exchange Using a Solution of 2 and 3 (6.5 mM) at Room Temperature. The intermolecular H_W/D_W exchange between a solution of **2** (6.5 mM) and **3** (6.3 mM) arrived at equilibrium within ca. 46 days giving **1** and **4**. For ^{31}P and ^{1}H NMR data, see section 2.1.

2.3. Double Label Crossover Experiment Probing H_W/D_W Exchange at −45 °C. A 0.016 M solution of **2** and a 0.022 M solution of **3** in toluene-d_8 were independently cooled to −70 °C. Then 0.3 mL of each solution of **2** and **3** was mixed in a Young tap NMR tube at −70 °C when NMR spectra were then recorded at various temperatures.

Shortly after the mixing at −70 °C (∼ 5 min) intermolecular exchange already started. After 35 min at −40 °C the reaction had nearly arrived at equilibrium.

^{1}H{^{31}P} NMR (500.0 MHz, toluene-h_8, −40 °C and −70 °C): **1**, δ −6.67 ppm (s, H_W); **3**, δ −6.73 ppm (s, H_W). For the ^{31}P NMR data of the four isotopomers, see section 2.1.

2.4. H/D Exchange Reaction in a Young Tap NMR Tube at 2 bar of D_2. In a Young tap NMR tube a 5.4 mM solution of **1** in hexane was pressurized with 2 bar of D_2. The reaction mixture was left at rt for 10 days. No exchange was observed based on the ^{31}P and ^{2}H NMR spectra recorded.

2.5. H/D Exchange Reaction under 60 bar of D_2 in an Autoclave. 3.3 mg of **1** were dissolved in 1 mL of toluene (5.4 mM) in an autoclave, which was pressurized with 60 bar of D_2 at 60 °C for 6 days. Traces of exchange were noticed, leading to the formation of **2**. ^{2}H NMR (76.6 MHz, toluene, rt): **2**, δ −6.62 ppm (multiplet, D_W).

2.6. H/D Exchange Reaction under 105 bar of D_2 in an Autoclave. 16.6 mg of **1** was dissolved in 1 mL of toluene (27.0 mM) in an autoclave, which was then pressurized with 105 bar of D_2 gas. The reaction mixture was stirred with a magnetic stirring bar at rt for 7 days. At the end of the reaction the remaining D_2 gas was slowly released under the protection of N_2 gas. Then an NMR sample was made of the reaction mixture for NMR measurements, which showed a complete H/D exchange between H_W of **1** and D_2 gas affording **2**. ^{2}H NMR (76.6 MHz, toluene, rt) δ −6.57 ppm (quintet, D_W).

3. H/D Exchange of 2 in Solution at 60 °C. In a Young tap NMR tube 10.0 mg of **2** was dissolved in 0.5 mL of toluene (32.5 mM). The sample was heated to 60 °C for 3 days. Then the exchange products were identified by ^{1}H, ^{2}H, and ^{31}P NMR spectroscopy.

^{1}H NMR (500.0 MHz, toluene-h_8, rt): **5d**, δ −5.88 ppm (quintet, H_W), 1.38 ppm (broad doublet, H_P−C_{H3}); **1.1md**, δ −6.62 ppm (quintet, Hw), 1.58 ppm (broad doublet, H_P−C_{H3}).

^{2}H NMR (76.7 MHz, toluene-h_8, rt): **7,** −5.83 ppm (quintet, D_W); **2**, −6.57 ppm (quintet, D_W); **1md**, 2.50 ppm (t, H_{CH_2D} of mesityl moiety), **5d**, 2.32 ppm (t, H_{CH_2D} of 2,3,5-trimethylphenyl moiety).

^{31}P NMR (202.5 MHz, toluene-h_8, rt): **7**, 23.83 ppm (t); **5d**, 23.86 ppm (s); **2**, 23.30 ppm (t); **1md**, 22.29 ppm (s); **5**, 23.83 ppm (s, partially overlap with **7**); **1**, 23.30 ppm (s, partially overlap with **2**).

4. Intramolecular H/D Exchange in the Solid State at 100 °C. 5 mg of **2** (red powder) were put into a Young NMR tube, and then the sample was heated at 100 °C for 2.5 h. After cooling to room temperature the sample was dissolved in 0.5 mL of toluene-h_8. A ^{31}P NMR spectrum showed that **1Pd** was formed.

^{1}H NMR (500.0 MHz, toluene-h_8, rt): δ −6.61 ppm (m, very weak, H_W).

^{2}H NMR (76.7 MHz, toluene-h_8, rt): δ 1.32 ppm (D_{CH_2D} of **1Pd**), −6.61 ppm (quintet, D_W of **2**).

^{31}P NMR (202.5 MHz, toluene-h_8, rt): **2**, δ 25.32 ppm (t); **1Pd**, δ 25.31 ppm (s).

5. X-ray Diffraction Study on 5. Crystals of **5** were grown under an atmosphere of dry nitrogen in a glovebox and embedded in polybutene oil. The only suitable crystal out of a manifold of very tiny thin needles was selected for the X-ray experiment by using a polarizing microscope and was mounted on the tip of a glass fiber and immediately transferred to the goniometer of an imaging-plate-detector system (Stoe IPDS diffractometer). The crystal was cooled to 183(2) K by using an Oxford Cryogenic system. In order to suppress a dominating number of unobserved intensity reflections, the crystal-to-image distance was set to 70 mm (θ_{max} = 25.88°) and the exposure time was set to 6.0 min per image, resulting in a ϕ-oscillation scan mode for the data collection. For the final cell parameter refinement, 8000 reflections were selected from the whole limiting sphere. A total of 10 799 diffraction intensities were collected,[27] of which 4983 were unique (R_{int} = 0.0823) after data reduction. 3247 of these reflections were considered observed by criterion $I > 2\sigma(I)$. A numerical absorption correction[28] based on eight crystal faces was applied with FACEitVIDEO and XRED.[27] The structure was solved by direct methods using the program SHELXS-

(27) Stoe IPDS software for data collection, cell refinement, and data reduction: Version 2.92 Stoe, Darmstadt, Germany, 1999.
(28) Coppens, P.; Leiserowitz, L.; Rabinovich, D. *Acta Crystallogr*. **1965**, *18*, 1035.

97.[29] Interpretation of the difference electron density maps, preliminary plot generations, and checking for higher symmetry were performed by using PLATON.[30] The full-matrix least-squares refinements (based on F^2) were carried out with SHELXL-97[31] using anisotropic displacement parameters for all non-hydrogen atoms, except for atoms C13, C16, and C17 which had to be refined isotropically due to nonpositive-definite anisotropic displacement parameters. This observation can be explained by many extreme tiny intergrown needles that contributed and probably overlapped some intensity data, adding systematic error to the absorption correction. The hydride H-atom position was interpreted from difference maps and its coordinates were fixed, but the isotropic displacement parameter was allowed to be refined. Positions of all other hydrogen atoms were calculated after each refinement cycle. The plot of the structure was generated by using ORTEP.[32]

Acknowledgment. Financial support for this work from the Swiss National Science Foundation and from the University of Zürich is gratefully acknowledged. Work at Los Alamos National Laboratory was supported by the Office of Science, U.S. Department of Energy.

Supporting Information Available: CCDC 627509 contains the supplementary crystallographic data for this paper. These data can be obtained free of charge from the Cambridge Crystallographic Data Centre via www.ccdc.cam.ac.uk/data_request/cif. ^{1}H and ^{2}H NMR spectra of the H/D exchange reaction according to Scheme 6. This material is available free of charge via Internet at http://pubs.acs.org.

JA069140K

(29) Sheldrick, G. M. *Acta Crystallogr., Sect. A* **1990**, *46*, 467.
(30) Spek, A. L. *J. Appl. Crystallogr.* **2003**, *36*, 7−13.
(31) Sheldrick, G. M. SHELXL-97: Software Package for Crystal Structure Determination and Refinement, University of Göttingen, Göttingen, Germany, 1997.
(32) Johnson, C. K. ORTEPII, Report ORNL-5138, Oak Ridge, Tennessee, U.S.A.